International Conference on Mathematics, Computational Methods & Reactor Physics (M&C 2009)
Saratoga Springs, New York, May 3-7, 2009, on CD-ROM, American Nuclear Society, LaGrange Park, IL (2009)

A DIFFUSION SYNTHETIC ACCELERATED LINEAR DISCONTINUOUS VERSION OF THE SPHERICAL GEOMETRY METHOD OF TUBES

Michael E. Rising
Department of Chemical and Nuclear Engineering
University of New Mexico
Albuquerque, New Mexico 87131-0001 USA
mrising1@unm.edu

Todd S. Palmer
Department of Nuclear Engineering and Radiation Health Physics
Oregon State University
Corvallis, Oregon 97331-4501 USA
palmerts@ne.orst.edu

ABSTRACT

There has been some interest in using 1-D spherical geometry transport discretizations for radiative transfer applications which often have very optically thick and diffusive physical properties. Previous work has involved the analysis and numerical testing of finite element methods (FEM) in various geometries in the optically thick and diffusive physical regime. We describe here the derivation and analysis of a new method, the Linear Discontinuous Method of Tubes (LDMOT) transport discretization. The asymptotic analysis predictions are corroborated with the results of several numerical test problems. The LDMOT behaves well in the thick, diffusive limit, with accurate results, because the leading order asymptotic diffusion equations are identical to the Linear Characteristic Method of Tubes (LCMOT) equations from a previous publication. We also describe a "Modified Four Step" diffusion synthetic acceleration (DSA) scheme that has been used to improve the convergence rate of the LDMOT method. Previous work has shown that the same acceleration scheme can be applied to methods that possess the same leading order asymptotic diffusion solution, and we have found that this scheme also accelerates the LCMOT scheme.

Key Words: Finite Element Method, Spherical Geometry, Diffusion Synthetic Acceleration

1. INTRODUCTION

The finite element method (FEM) has long been applied to the spatial (and angular) discretization of the radiative transfer equation for many years. In this approach, the fundamental unknown is expanded in a finite set of known basis functions of the independent variable of interest. The coefficients of the expansion are determined from a set of weighted residual equations formulated by integrating the transport equation with a set of known weight functions. The choice of weight and basis functions, and the subspace of the domain over which they are defined, uniquely determine the discretization.

The most common approach to the solution of the spherical geometry transport equation involves independent discretizations of the angular and radial variables. The angular variable is often

treated with weighted diamond differencing (WDD) [13], allowing the spatial variable to be treated with WDD, the finite element method, or any other method of interest. Certain finite element schemes, in conjunction with WDD in angle, have been shown to yield accurate solutions in thick, diffusive regions [1]. WDD-in-angle has the disadvantage that there is a serial ordering of the angular variable: from $\mu = -1$ (the starting direction) through the quadrature set from μ_{min} to μ_{max}. Recently, Warsa and Morel [2] have developed a P_{N-1} - equivalent S_N angular discretization that avoids the need for the solution of a "starting direction" transport equation, and yields accurate results in thick diffusive regions.

In a recent paper [5], we developed a 1-D spherical geometry moments-based linear characteristic version of the method of tubes" (MOT) described by Nikoforova et al [3]. The streaming operator of the spherical geometry transport equation is transformed into a simple derivative along the direction of particle flow. In this transformed coordinate system, any 1-d Cartesian geometry transport discretization can be implemented. Furthermore, the solution of a starting direction is unnecessary, and the solution can be obtained in each "tube" in the problem *in parallel*. A linear characteristic (LCMOT) version of the scheme was predicted and observed to behave very well in thick diffusive regions.

In this paper, we show that in this transformed coordinate system, a linear discontinuous FEM can be employed with excellent results. This *new* version of the method of tubes is a variant of the traditional slab geometry linear discontinuous (LD) FEM, written in "slope and average" notation. We have performed an asymptotic analysis of this new method to predict its behavior in optically thick and diffusive regions and have confirmed the predictions of this analysis by solving several numerical test problems.

The remainder of this paper contains the spherical geometry transport equation transformed to a characteristic form and a derivation of the LD discretization. We show the results of the asymptotic analysis and derive a diffusion synthetic acceleration (DSA) scheme for this method. A suite of test problems has been defined and solved, including several problems in the optically thick and diffusive limit, and the results indicate that the method works very well.

2. THE SPHERICAL GEOMETRY TRANSPORT EQUATION

The transport equation for spherical geometry in (r, μ) notation has the following conservative form:

$$\frac{\mu}{r^2}\frac{\partial}{\partial r}[r^2\psi(r,\mu)] + \frac{1}{r}\frac{\partial}{\partial \mu}[(1-\mu^2)\psi(r,\mu)] + \sigma_t(r)\psi(r,\mu) = \frac{1}{2}\sigma_s(r)\int_{-1}^{1}\psi(r,\mu')d\mu' + \frac{1}{2}q(r)\,, \quad 0 \le r \le R,\ -1 \le \mu \le 1\,, \tag{1}$$

with a specified incident angular flux outer boundary condition:

$$\psi(R,\mu) = \psi^{in}(\mu)\,, \qquad \mu < 0\,. \tag{2}$$

Eqs. (1) and (2) can be transformed into a characteristic form,

$$\frac{d}{d\ell}\psi(\ell) + \sigma(\ell)\psi(\ell) = \frac{1}{2}\sigma_s(\ell)\phi(\ell) + \frac{1}{2}q(\ell)\,, \tag{3}$$

where we have made use of the following relationship,

$$\frac{d\psi}{d\ell} = \frac{\partial r}{\partial \ell}\frac{\partial \psi}{\partial r} + \frac{\partial \mu}{\partial \ell}\frac{\partial \psi}{\partial \mu}\,. \tag{4}$$

As a consequence of this relationship, the characteristic curves along the direction of particle travel are defined as a constant, c,

$$c = r\sqrt{1-\mu^2}\,. \tag{5}$$

Given the transport equation in ℓ-space and the constant which defines the tube boundaries given in Eq. (5) we can introduce the space-angle grid shown in Fig. 1. A *tube* (the shaded area in Figure 1 is numbered with integer index t, and is defined as the phase space volume between two characteristic curves: the curve that intersects μ=0 at $r_{t-1/2}$ and the curve that intersects μ=0 at $r_{t+1/2}$. Notice that the angular mesh is completely determined given a choice of spatial mesh. The number of angular intervals at large radii is twice the number of radial mesh cells in the problem, and as $r \rightarrow 0$ the number of angular intervals is two. For spherical systems with N_r cells in the radial dimension there are $N_r\,(N_r+1)$ space-angle cells. Also, given a uniform spacing in radius, the angular mesh will be nonuniform (see Figure 1).

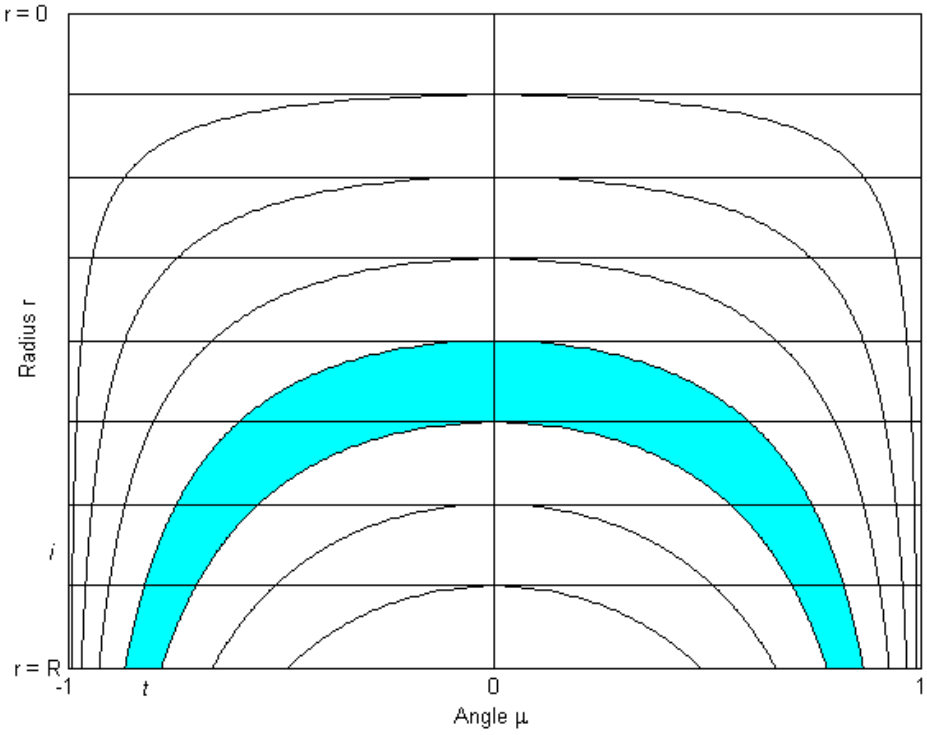

Figure 1. The Space-Angle Grid for the Method of Tubes

Fig. 2 illustrates the phase-space cell (t,i) that is the fundamental volume used in the MOT discretizations. The average characteristic path length within the volume element (t,i) is $\Delta\ell_{t,i}$. The volume of a phase-space element (t,i) is defined as $\Delta_{t,i}$ and the volume of a radial shell i is defined as ΔV_i. Similar to S_N methods, we calculate the radial average scalar flux and scalar flux

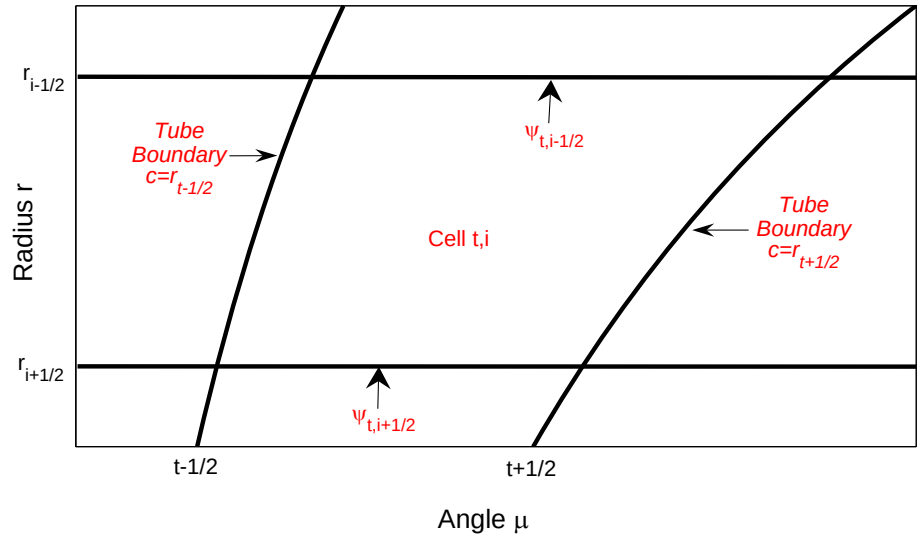

Figure 2. A Blowup of Space-Angle Mesh Cell (t, i) in the Method of Tubes

slope by summing over the angular fluxes multiplied by an ordinate weight. In the Method of Tubes, the ratio of the volume of cell (t, i) to the volume of the radial shell i, $\left(\frac{\Delta_{t,i}}{\Delta V_i}\right)$, is used to calculate the spatial average and slope of the scalar flux from the average and slope of the angular flux in the cell:

$$\phi_i = \sum_t \psi_{t,i} \frac{\Delta_{t,i}}{\Delta V_i} \,, \tag{6}$$

$$\phi_i^x = \sum_t \psi_{t,i}^x \frac{\Delta_{t,i}}{\Delta V_i} \,, \tag{7}$$

[A complete derivation of these quantities is available in previous publications [3, 5].]

3. THE LINEAR DISCONTINUOUS METHOD OF TUBES (LDMOT)

Previous discretizations of the Method of Tubes include some approximate slope characteristic methods [3] and some more recent moment-based characteristic methods [4, 5]. Here we present a *new* discretization applied to the MOT derived from the concepts of the slab geometry linear discontinuous FEM. We define the basis functions for LDMOT such that they approximate the solution as linear on the interval from 0 to $\Delta\ell_{t,i}$:

$$\psi(\ell) = \psi_L b_L(\ell) + \psi_R b_R(\ell) \,, \quad Q(\ell) = Q_L b_L(\ell) + Q_R b_R(\ell) \,, \tag{8}$$

where,

$$Q_R = \sigma_s \phi_R + q_R \,, \quad Q_L = \sigma_s \phi_L + q_L \,, \tag{9}$$

and,

$$b_R(\ell) = \frac{\ell}{\Delta\ell_{t,i}} \,, \quad b_L(\ell) = \frac{\Delta\ell_{t,i} - \ell}{\Delta\ell_{t,i}} \,. \tag{10}$$

Notice that by substituting the basis function expansions of the solution and source into our governing transport equation (Eq. (1)), we have a single equation for two unknowns (ψ_L and ψ_R) for each cell. Following the original LD slab geometry methodology, we form two weighted residual equations by multiplying the governing equation by each of the linear basis functions in Eq. (10). and integrating over a spatial cell:

$$\int_0^{\Delta\ell_{t,i}} w_j(\ell)\left[\frac{\partial\psi(\ell)}{\partial\ell}+\sigma_i\psi(\ell)\right]d\ell=\frac{1}{2}\int_0^{\Delta\ell_{t,i}} w_j(\ell)Q(\ell)\,d\ell\,,\quad j=1,2\quad, \tag{11}$$

where,

$$w_1(\ell)=\frac{\ell}{\Delta\ell_{t,i}}\,,\quad w_2(\ell)=\frac{\Delta\ell_{t,i}-\ell}{\Delta\ell_{t,i}}\,. \tag{12}$$

Evaluating Eq. (11) for both weighting functions and substituting the basis function expansions (Eq. (8)) , we obtain the LDMOT discretized equations:

$$\begin{aligned}&\left[\frac{\psi_{t,Li}+\psi_{t,Ri}}{2}-\psi_{t,i-1/2}\right]+\sigma_i\Delta\ell_{t,i}\left[\frac{\psi_{t,Li}}{3}+\frac{\psi_{t,Ri}}{6}\right]\\&\quad=\frac{\Delta\ell_{t,i}}{2}\left[\frac{Q_{Li}}{3}+\frac{Q_{Ri}}{6}\right],\end{aligned} \tag{13}$$

$$\begin{aligned}&\left[\psi_{t,i+1/2}-\frac{\psi_{t,Li}+\psi_{t,Ri}}{2}\right]+\sigma_i\Delta\ell_{t,i}\left[\frac{\psi_{t,Li}}{6}+\frac{\psi_{t,Ri}}{3}\right]\\&\quad=\frac{\Delta\ell_{t,i}}{2}\left[\frac{Q_{Li}}{6}+\frac{Q_{Ri}}{3}\right],\end{aligned} \tag{14}$$

where an upstream closure is used for cell-edge angular fluxes:

$$\psi_{t,i-1/2}=\begin{cases}\psi_t^*, & \mu_t>0,\quad i=t\,,\\ \psi_{t,Li}, & \mu_t<0,\quad t<i\le I\,,\end{cases} \tag{15}$$

$$\psi_{t,i+1/2}=\begin{cases}\psi_{t,inc}, & \mu_t<0,\quad i=I\,,\\ \psi_{t,Ri}, & \mu_t>0,\quad t\le i<I\,.\end{cases} \tag{16}$$

The LDMOT equations in the familiar "slope and average" form are:

$$\psi_{t,i}=\frac{\psi_{t,Ri}+\psi_{t,Li}}{2}\,,\quad \psi_{t,i}^x=\frac{\psi_{t,Ri}-\psi_{t,Li}}{2}\,, \tag{17}$$

leading to,

$$\frac{[\psi_{t,i+1/2} - \psi_{t,i-1/2}]}{\Delta\ell_{t,i}} + \sigma_i \psi_{t,i} = \frac{1}{2}[\sigma_{si}\phi_i + q_i]\,, \tag{18}$$

$$\frac{3[\psi_{t,i+1/2} + \psi_{t,i-1/2} - 2\psi_{t,i}]}{\Delta\ell_{t,i}} + \sigma_i \psi^x_{t,i} = \frac{1}{2}[\sigma_{si}\phi^x_i + q^x_i]\,, \tag{19}$$

where the closure for cell-edge angular fluxes is,

$$\psi_{t,i-1/2} = \begin{cases} \psi^*_t, & \mu_t > 0, \quad i = t\,, \\ \psi_{t,i} - \psi^x_{t,i}, & \mu_t < 0, \quad t < i \le I\,, \end{cases} \tag{20}$$

$$\psi_{t,i+1/2} = \begin{cases} \psi_{t,inc}, & \mu_t < 0, \quad i = I\,, \\ \psi_{t,i} + \psi^x_{t,i}, & \mu_t > 0, \quad t \le i < I\,. \end{cases} \tag{21}$$

[Note the ψ^*_t in Eqs. (15) and (20) is known due to the reflecting boundary conditions in each of the tubes at $\mu_t = 0$.]

4. ASYMPTOTIC ANALYSIS OF THE ANALYTIC SPHERICAL GEOMETRY TRANSPORT EQUATION (REVIEW)

It has long been known that transport theory transitions to diffusion theory under certain conditions. The process used to mathematically confirm this conjecture is known as an "asymptotic analysis" and has been illustrated in many places in the literature[6, 7]. This technique involves a scaling of the transport equation by a small parameter ε. This scaling mathematically details the special group of problems with which we are concerned; namely optically thick ($\frac{\sigma_t}{\varepsilon} \gg 1$) and diffusive ($\varepsilon\sigma_a \ll 1$) problems. Applying this scaling to Eqs. (1) and (2) yields,

$$\frac{\mu}{r^2}\frac{\partial}{\partial r}[r^2\psi(r,\mu)] + \frac{1}{r}\frac{\partial}{\partial \mu}[(1-\mu^2)\psi(r,\mu)] + \frac{\sigma_t(r)}{\varepsilon}\psi(r,\mu) = \frac{1}{2}\left(\frac{\sigma_t(r)}{\varepsilon} - \varepsilon\sigma_a(r)\right)\int_{-1}^{1}\psi(r,\mu')d\mu' + \frac{1}{2\varepsilon}q(r)\,,$$

$$0 \le r \le R, \quad -1 \le \mu \le 1\,, \tag{22}$$

$$\psi(R,\mu) = \psi^{in}(\mu)\,, \qquad \mu < 0\,. \tag{23}$$

We observe the behavior of the transport solution as ε tends toward zero. Introducing power series expansions for both the angular and scalar fluxes,

$$\psi(r,\mu) = \psi^{[0]}(r,\mu) + \varepsilon\psi^{[1]}(r,\mu) + \varepsilon^2\psi^{[2]}(r,\mu) + \ldots\,, \tag{24}$$

$$\phi(r) = \psi^{[0]}(r) + \varepsilon\phi^{[1]}(r) + \varepsilon^2\phi^{[2]}(r) + \ldots, \tag{25}$$

we find that in the interior of the diffusive region, the leading-order angular flux is *isotropic* and satisfies a *diffusion equation*:

$$\psi(r,\mu) = \frac{1}{2}\,\phi(r) + O(\varepsilon), \tag{26}$$

$$-\frac{1}{r^2}\frac{d}{dr}\left(\frac{r^2}{3\sigma_t(r)}\frac{d\phi(r)}{dr}\right) + \sigma_a(r)\phi(r) = q(r), \tag{27}$$

with "transport-corrected" boundary conditions

$$\phi(R) = 2\int_{-1}^{0} d\mu\; W(|\mu|)\psi^{in}(\mu). \tag{28}$$

Equation (28) is a Dirichlet boundary condition equal to a weighted integral of the incoming angular flux on the outer surface of the sphere $\psi^{in}(\mu)$. The weight function $W(\mu)$ is defined in terms of Chandrasekhar's H function for a purely scattering medium[8]:

$$\begin{aligned} W(\mu) &= \frac{\sqrt{3}}{2}\mu H(\mu) \\ &= 0.91\mu + 1.635\mu^2 \pm \text{a few \%} \\ &\approx \mu + \frac{3}{2}\mu^2. \end{aligned} \tag{29}$$

This asymptotic analysis has long been used as a tool to determinine whether *discretized* transport equations transition to accurate *discretized* diffusion equations (with accurate boundary conditions) in thick diffusive regions. If so, and if the spatial grid is fine enough to resolve the diffusion solution, we claim that the transport discretization is accurate in these regions.

5. ASYMPTOTIC ANALYSIS OF LDMOT

In this section, we use the asymptotic analysis described in the previous section to predict the behavior of the LDMOT scheme in optically thick and diffusive regions. We apply the asymptotic analysis and determine whether the solution of the discrete transport equations in the interior of thick diffusive regions (to leading order) satisfies a discrete diffusion equation. The boundary conditions which constrain the interior solution can also be obtained. If the discretized transport equations in these optically thick and diffusive regions yield accurate discretizations of the

diffusion equations with accurate boundary conditions, then we say that the transport method is well-behaved in the thick, diffusion limit.

If we introduce the appropriate scaling of cross sections and source, and expand the angular and scalar flux solutions in power series in ε

$$\psi = \sum_{m=0}^{\infty} \varepsilon^m \psi^{[m]}, \quad \phi = \sum_{m=0}^{\infty} \varepsilon^m \phi^{[m]}, \tag{30}$$

equating the coefficients of the various powers of ε yields information about the leading order LDMOT solution in diffusive regions.

Beginning with the average-slope form of the LDMOT equations (Eqs. (18), (19), (20) and (21)), we obtain the following equations: $O(\varepsilon^{-1})$:

$$\psi_{t,i}^{[0]} = \frac{1}{2}\phi_i^{[0]}, \tag{31}$$

$$\psi_{t,i}^{x[0]} = \frac{1}{2}\phi_i^{x[0]}. \tag{32}$$

$O(1)$:

$$\frac{\psi_{t,i+1/2}^{[0]} - \psi_{t,i-1/2}^{[0]}}{\Delta\ell_{t,i}} + \sigma_i \psi_{t,i}^{[1]} = \frac{\sigma_i}{2}\phi_i^{[1]}, \tag{33}$$

$$\frac{3[\psi_{t,i+1/2}^{[0]} + \psi_{t,i-1/2}^{[0]} - 2\psi_{t,i}^{[0]}]}{\Delta\ell_{t,i}} + \sigma_i \psi_{t,i}^{x[1]} = \frac{\sigma_i}{2}\phi_i^{x[1]}, \tag{34}$$

$$\psi_{t,i+1/2}^{[0]} = \psi_{t,i}^{[0]} + \psi_{t,i}^{x[0]} = \frac{1}{2}(\phi_i^{[0]} + \phi_i^{x[0]}), \quad \Delta\ell_{t,i} > 0, \tag{35}$$

$$\psi_{t,i-1/2}^{[0]} = \psi_{t,i}^{[0]} - \psi_{t,i}^{x[0]} = \frac{1}{2}(\phi_i^{[0]} - \phi_i^{x[0]}), \quad \Delta\ell_{t,i} < 0. \tag{36}$$

$O(\varepsilon)$:

$$\frac{\psi_{t,i+1/2}^{[1]} - \psi_{t,i-1/2}^{[1]}}{\Delta\ell_{t,i}} + \sigma_i \psi_{t,i}^{[2]} = \frac{\sigma_i}{2}\phi_i^{[2]} - \frac{\sigma_{ai}}{2}\phi_i^{[0]} + \frac{1}{2}q_i, \tag{37}$$

$$\frac{3[\psi_{t,i+1/2}^{[1]} + \psi_{t,i-1/2}^{[1]} - 2\psi_{t,i}^{[1]}]}{\Delta\ell_{t,i}} + \sigma_i \psi_{t,i}^{x[2]} = \frac{\sigma_i}{2}\phi_i^{x[2]} - \frac{\sigma_{ai}}{2}\phi_i^{x[0]} + \frac{1}{2}q_i^x. \tag{38}$$

A comparison of this set of eight equations with those from the linear characteristic method of tubes (LCMOT) [5] shows that the leading order solutions from the two methods satisfy the same leading order discretized diffusion equations,

$$\begin{aligned} -\frac{1}{2\sigma_{i+1}}(\Phi_{i+3/2} - \Phi_{i+1/2}) \sum_t \frac{\Delta_{t,i+1}}{\Delta\ell_{t,i+1}^2} + \frac{1}{2\sigma_i}(\Phi_{i+1/2} - \Phi_{i-1/2}) \sum_t \frac{\Delta_{t,i}}{\Delta\ell_{t,i}^2} \\ + \frac{1}{4}[\sigma_{ai}\Delta V_i(\frac{4}{3}\Phi_{i+1/2} + \frac{2}{3}\Phi_{i-1/2}) + \sigma_{ai+1}\Delta V_{i+1}(\frac{4}{3}\Phi_{i+1/2} + \frac{2}{3}\Phi_{i+3/2})], \quad 1 \le i \le I, \\ = \frac{1}{2}[\Delta V_i(q_i + \frac{1}{3}q_i^x) + \Delta V_{i+1}(q_{i+1} - \frac{1}{3}q_{i+1}^x)] \end{aligned} \tag{39}$$

and,

$$\Phi_{i+1/2} = \phi^{[0]}_{i+1/2}\,, \quad 1 \le i < I\,, \tag{40}$$

$$\frac{1}{2}\Phi_{I+1/2} = \frac{1}{\gamma_I - \alpha_I} \sum_{\Delta\ell_t, I>0} \left[(\gamma_I - 2\alpha_I) \frac{\Delta\ell^{-1}_{t,I}}{\rho_I} + \frac{3\Delta\ell^{-2}_{t,I}}{2} \right] g_t \Delta_{t,I}\,, \tag{41}$$

where,

$$\begin{aligned} \gamma_I &= \frac{3}{2} \sum_t \frac{\Delta_{t,I}}{\Delta\ell^2_{t,I}} \\ \alpha_I &= \frac{1}{2}\sigma_I \sigma_{aI} \Delta V_I \end{aligned} \tag{42}$$

Eqs. ((39)-(42)) show that the LDMOT will generate accurate solutions in thick diffusive regions. The outer boundary condition on the leading order interior solution is a discrete version of the $\mu + \frac{3}{2}\mu^2$ weighted integral of the incoming angular flux - a result from the asymptotic analysis of the analytic spherical geometry transport equation. The three-point removal may introduce unphysical oscillations in the solution. A "lumping" procedure may be used to improve the robustness of the method at the cost of a reduction in accuracy.

6. DIFFUSION SYNTHETIC ACCELERATION OF LDMOT

In radiative transfer simulations employing source iteration (SI), a preconditioner or accelerator is required to efficiently generate solutions in optically thick and diffusive media. An efficient acceleration scheme is one that increases the *rate* of convergence (compared with the unaccelerated method), reducing the spectral radius and reducing the likelihood of false convergence. In this research we have chosen to implement a version of "Modified 4-Step" Diffusion Synthetic Acceleration (DSA) [9].

After a transport sweep has been completed (index $(l + 1/2)$) we can define "corrections", that if available, would yield the converged solution to the transport problem:

$$f_t(r) = \psi_t^{\text{converged}}(r) - \psi_t^{(l+1/2)}(r)\,, \tag{43}$$

$$F_t(r) = \phi_t^{\text{converged}}(r) - \phi_t^{(l+1/2)}(r)\,. \tag{44}$$

We generate exact equations for these corrections by subtracting the iteration equations in right-left form (Eqs. (13-16)) from the converged equations:

$$\begin{aligned} &\left[\frac{f_{t,Li} + f_{t,Ri}}{2} - f_{t,i-1/2} \right] + \sigma_i \Delta\ell_{t,i} \left[\frac{f_{t,Li}}{3} + \frac{f_{t,Ri}}{6} \right] - \frac{\sigma_{si}\Delta\ell_{t,i}}{2} \left[\frac{F_{Li}}{3} + \frac{F_{Ri}}{6} \right] \\ &\quad = \frac{\sigma_{si}\Delta\ell_{t,i}}{2} \left[\frac{\phi^{(l+1/2)}_{Li} - \phi^{(l)}_{Li}}{3} + \frac{\phi^{(l+1/2)}_{Ri} - \phi^{(l)}_{Ri}}{6} \right], \end{aligned} \tag{45}$$

$$\left[f_{t,i+1/2} - \frac{f_{t,Li} + f_{t,Ri}}{2}\right] + \sigma_i \Delta\ell_{t,i}\left[\frac{f_{t,Li}}{6} + \frac{f_{t,Ri}}{3}\right] - \frac{\sigma_{si}\Delta\ell_{t,i}}{2}\left[\frac{F_{Li}}{6} + \frac{F_{Ri}}{3}\right] = \frac{\sigma_{si}\Delta\ell_{t,i}}{2}\left[\frac{\phi_{Li}^{(l+1/2)} - \phi_{Li}^{(l)}}{6} + \frac{\phi_{Ri}^{(l+1/2)} - \phi_{Ri}^{(l)}}{3}\right], \tag{46}$$

where index (l) and $(l + 1/2)$ in the source refer to the values before the source iteration and after source iteration, respectively. The closure conditions for the angular flux corrections are:

$$f_{t,i-1/2} = \begin{cases} f_t^*, & \mu_t > 0, \quad i = t\,, \\ f_{t,Li}, & \mu_t < 0, \quad t < i \leq I\,, \end{cases} \tag{47}$$

$$f_{t,i+1/2} = \begin{cases} f_{t,inc}, & \mu_t < 0, \quad i = I\,, \\ f_{t,Ri}, & \mu_t > 0, \quad t \leq i < I\,. \end{cases} \tag{48}$$

In the Modified Four-Step (M4S) procedure, we

A. Calculate the zero-th and first angular moments of the discretized transport equation for LDMOT.

B. Change the iteration indices to l + 1, except on the second and higher moment terms to obtain acceleration equations.

C. Subtract the acceleration equations from the unaccelerated equations to reduce algebraic complexity.

D. Eliminate the first angular flux moments from the resulting system, leaving discretized diffusion equations for the scalar fluxes.

We introduce the P_1 approximation to make the correction equations more efficient to solve:

$$f_t(r) = \frac{1}{2}(F(r) + 3\mu_t(r)G(r))\,, \tag{49}$$

where $G(r)$ is defined as the net current correction at a position r. We use this approximation to simplify some of the terms in the first angular moment of the discretized transport equation.

To this point, we have performed the exact steps associated with the original four-step procedure of Larsen [12]. Instead of taking the first angular moment of Eqs. (47) and (48) we use an approximate closure for the scalar fluxes. The significant difference in the M4S procedure is in this closure approximation:

$$F_{i-1/2} = F_{Li}\,, \tag{50}$$

$$F_{i+1/2} = F_{Ri}\,. \tag{51}$$

After much algebraic manipulation we obtain two DSA equation for each interior cell:

$$
\begin{aligned}
&\left[\frac{1}{2\sigma_i}\sum_t \frac{\Delta_{t,i}}{\Delta\ell_{t,i}^2}\left(1-\frac{\sum\limits_{\Delta\ell_{t,i}>0}\frac{\mu_{t,i-1/2}\Delta_{t,i}}{\Delta\ell_{t,i}}}{\sum\limits_t \frac{\mu_{t,i-1/2}\Delta_{t,i}}{\Delta\ell_{t,i}}}\right)+\frac{1}{2}\sum_{\Delta\ell_{t,i}>0}\frac{\Delta_{t,i}}{\Delta\ell_{t,i}}+\frac{1}{3}\sigma_{ai}\Delta V_i\right]F_{Li}\\
&+\left[\frac{1}{2\sigma_i}\sum_t \frac{\Delta_{t,i}}{\Delta\ell_{t,i}^2}\left(\frac{\sum\limits_{\Delta\ell_{t,i}>0}\frac{\mu_{t,i-1/2}\Delta_{t,i}}{\Delta\ell_{t,i}}}{\sum\limits_t \frac{\mu_{t,i-1/2}\Delta_{t,i}}{\Delta\ell_{t,i}}}-1\right)+\frac{1}{6}\sigma_{ai}\Delta V_i\right]F_{Ri}\\
&+\left[\frac{1}{2\sigma_{i-1}}\sum_t \frac{\Delta_{t,i-1}}{\Delta\ell_{t,i-1}^2}\left(\frac{\sum\limits_{\Delta\ell_{t,i}>0}\frac{\mu_{t,i-1/2}\Delta_{t,i}}{\Delta\ell_{t,i}}}{\sum\limits_t \frac{\mu_{t,i-1/2}\Delta_{t,i-1}}{\Delta\ell_{t,i-1}}}\right)-\frac{1}{2}\sum_{\Delta\ell_{t,i}>0}\frac{\Delta_{t,i}}{\Delta\ell_{t,i}}\right]F_{Ri-1}\\
&+\left[-\frac{1}{2\sigma_{i-1}}\sum_t \frac{\Delta_{t,i-1}}{\Delta\ell_{t,i-1}^2}\left(\frac{\sum\limits_{\Delta\ell_{t,i}>0}\frac{\mu_{t,i-1/2}\Delta_{t,i}}{\Delta\ell_{t,i}}}{\sum\limits_t \frac{\mu_{t,i-1/2}\Delta_{t,i-1}}{\Delta\ell_{t,i-1}}}\right)\right]F_{Li-1}\\
&=\sigma_{si}\Delta V_i\left[\frac{\phi_{Li}^{(l+1/2)}-\phi_{Li}^{(l)}}{3}+\frac{\phi_{Ri}^{x(l+1/2)}-\phi_{Ri}^{x(l)}}{6}\right],\qquad 1<i\le I\,,
\end{aligned}
\tag{52}
$$

$$
\begin{aligned}
&\left[\frac{1}{2\sigma_i}\sum_t \frac{\Delta_{t,i}}{\Delta\ell_{t,i}^2}\left(1-\frac{\sum\limits_{\Delta\ell_{t,i}>0}\frac{\mu_{t,i+1/2}\Delta_{t,i}}{\Delta\ell_{t,i}}}{\sum\limits_t \frac{\mu_{t,i+1/2}\Delta_{t,i}}{\Delta\ell_{t,i}}}\right)+\frac{1}{2}\sum_{\Delta\ell_{t,i}>0}\frac{\Delta_{t,i}}{\Delta\ell_{t,i}}+\frac{1}{3}\sigma_{ai}\Delta V_i\right]F_{Ri}\\
&+\left[\frac{1}{2\sigma_i}\sum_t \frac{\Delta_{t,i}}{\Delta\ell_{t,i}^2}\left(\frac{\sum\limits_{\Delta\ell_{t,i}>0}\frac{\mu_{t,i+1/2}\Delta_{t,i}}{\Delta\ell_{t,i}}}{\sum\limits_t \frac{\mu_{t,i+1/2}\Delta_{t,i}}{\Delta\ell_{t,i}}}-1\right)+\frac{1}{6}\sigma_{ai}\Delta V_i\right]F_{Li}\\
&+\left[\frac{1}{2\sigma_{i+1}}\sum_t \frac{\Delta_{t,i+1}}{\Delta\ell_{t,i+1}^2}\left(\frac{\sum\limits_{\Delta\ell_{t,i}>0}\frac{\mu_{t,i+1/2}\Delta_{t,i}}{\Delta\ell_{t,i}}}{\sum\limits_t \frac{\mu_{t,i+1/2}\Delta_{t,i+1}}{\Delta\ell_{t,i+1}}}\right)-\frac{1}{2}\sum_{\Delta\ell_{t,i}>0}\frac{\Delta_{t,i}}{\Delta\ell_{t,i}}\right]F_{Li+1}\\
&+\left[-\frac{1}{2\sigma_{i+1}}\sum_t \frac{\Delta_{t,i+1}}{\Delta\ell_{t,i+1}^2}\left(\frac{\sum\limits_{\Delta\ell_{t,i}>0}\frac{\mu_{t,i+1/2}\Delta_{t,i}}{\Delta\ell_{t,i}}}{\sum\limits_t \frac{\mu_{t,i+1/2}\Delta_{t,i+1}}{\Delta\ell_{t,i+1}}}\right)\right]F_{Ri+1}\\
&=\sigma_{si}\Delta V_i\left[\frac{\phi_{Li}^{(l+1/2)}-\phi_{Li}^{(l)}}{6}+\frac{\phi_{Ri}^{x(l+1/2)}-\phi_{Ri}^{x(l)}}{3}\right],\qquad 1\le i<I\,.
\end{aligned}
\tag{53}
$$

We now have $2(I-1)$ equations for $2I$ unknowns. Equations for the outer boundary condition

and the inner reflecting boundary ($r = 0$). First, we apply the reflecting inner boundary condition with:

$$\sum_t f_{t,1/2} \frac{\Delta_{t,1}}{\Delta \ell_{t,1}} = 0 \,. \tag{54}$$

We obtain the correction equation for the interior edge:

$$\begin{aligned} &\left[\frac{1}{2\sigma_1} \sum_t \frac{\Delta_{t,1}}{\Delta \ell_{t,1}^2} + \frac{1}{3} \sigma_{a1} \Delta V_i \right] F_{L1} + \left[\frac{1}{2\sigma_1} \sum_t \frac{\Delta_{t,1}}{\Delta \ell_{t,1}^2} + \frac{1}{6} \sigma_{a1} \Delta V_1 \right] F_{R1} \\ &\quad = \sigma_{s1} \Delta V_1 \left[\frac{\phi_{L1}^{(l+1/2)} - \phi_{L1}^{(l)}}{3} + \frac{\phi_{R1}^{x(l+1/2)} - \phi_{R1}^{x(l)}}{6} \right] . \end{aligned} \tag{55}$$

We use the outer boundary condition in Eq. (48) and formulate an equation for the outermost cell:

$$\begin{aligned} &\left[\frac{1}{2\sigma_I} \sum_t \frac{\Delta_{t,I}}{\Delta \ell_{t,I}^2} \left(1 - \frac{\sum_{\Delta \ell_{t,I} > 0} \frac{\mu_{t,I+1/2} \Delta_{t,I}}{\Delta \ell_{t,I}}}{\sum_t \frac{\mu_{t,I+1/2} \Delta_{t,I}}{\Delta \ell_{t,I}}} \right) + \frac{1}{2} \sum_{\Delta \ell_{t,I} > 0} \frac{\Delta_{t,I}}{\Delta \ell_{t,I}} + \frac{1}{3} \sigma_{aI} \Delta V_I \right] F_{RI} \\ &\quad + \left[\frac{1}{2\sigma_I} \sum_t \frac{\Delta_{t,I}}{\Delta \ell_{t,I}^2} \left(\frac{\sum_{\Delta \ell_{t,I} > 0} \frac{\mu_{t,I+1/2} \Delta_{t,I}}{\Delta \ell_{t,I}}}{\sum_t \frac{\mu_{t,I+1/2} \Delta_{t,I}}{\Delta \ell_{t,I}}} - 1 \right) + \frac{1}{6} \sigma_{aI} \Delta V_I \right] F_{LI} \\ &\quad = \sigma_{sI} \Delta V_I \left[\frac{\phi_{LI}^{(l+1/2)} - \phi_{LI}^{(l)}}{6} + \frac{\phi_{RI}^{x(l+1/2)} - \phi_{RI}^{x(l)}}{3} \right] . \end{aligned} \tag{56}$$

This $2I \times 2I$ linear system of equations is solved using a banded matrix solver to determine scalar flux corrections.

Adams et al [10] showed that if a finite element method (FEM) has the same asymptotic diffusion limit as a particular characteristic method, the DSA scheme developed for the FEM can be applied to the CM. Using this concept, we have successfully used the DSA scheme described here to accelerate the LCMOT transport iterations [5].

7. NUMERICAL RESULTS

We have implemented the LDMOT discretization and have solved several test problems to observe the behavior of these methods in a variety of physical regimes.

7.1. Reed's Test

The spherical geometry version of the Reed problem [11] is a good test of a transport method because it involves spatial regions with a variety of different transport physics: a thick absorber with a source, a thin absorber, a void region, a thin scatterer with a source, and a source-free thin scatterer. This problem does not contain optically thick, diffusive regions; we run this problem as a way of testing the implementation of the transport methods. Table I contains the Reed test problem material and mesh specification. The LDMOT result is compared to a weighted-diamond in angle, "fully-lumped" linear discontinuous (LD) finite element in space solution [1].

Table I. Test Problem 1

Region	Spatial Interval	# of Spatial Intervals	σ_t	σ_s	q
1	$0 < r < 2$	10	50	0	50
2	$2 < r < 3$	5	5	0	0
3	$3 < r < 5$	10	0	0	0
4	$5 < r < 6$	5	1	0.9	0.7
5	$6 < r < 8$	10	1	0.9	0

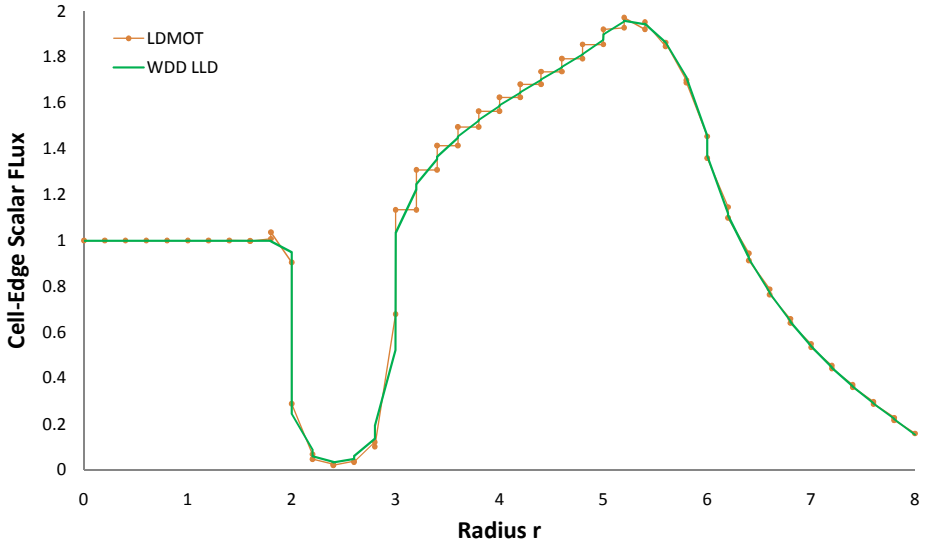

Figure 3. Test Problem 1 Cell-Edge Scalar Flux Solutions for the LDMOT and "Fully-Lumped" LD Schemes

Figure 3 shows that the LDMOT scheme compares well with the reference finite element calculation.

7.2. A Test with a Diffusive Region

In this test problem, we consider a two-region sphere with a vacuum outer boundary ($R = 20$) [7]: a central region with a source surrounded by an optically thick, purely scattering outer region. The purpose of this test problem is to investigate the quality of the differencing of the diffusion operator in the optically thick and diffusive regions. [There is no impact of the three-point removal term in this problem, though, because there is no absorption in the diffusive region.] The spatial mesh is uniform and has 20 cells. The specification of this test problem is shown in Table II. The infinite medium solution in the central region is

$$\phi(r) = \phi_\infty(r) = \frac{q}{\sigma_a} = 1\,, \tag{57}$$

and at the interface between the two regions, the transport scalar flux approaches the solution of the diffusion problem

$$\begin{aligned} -\frac{1}{r^2}\frac{\partial}{\partial r} r^2 D \frac{\partial \phi}{\partial r} &= 0\,, \\ \phi(10) = \phi_\infty(10)\,, \qquad \phi(20) &= 0\,. \end{aligned} \tag{58}$$

The solution in the outer region is

$$\phi(r) = \phi_\infty(10)\left(\frac{20}{r} - 1\right)\,. \tag{59}$$

Table II. Test Problem 2

Region	Spatial Interval	σ_t	σ_s	q
1	$0 < r < 10$	100	90	10
2	$10 < r < 20$	100	100	0

Figure 4 illustrates the solution of this problem for the LDMOT scheme. This method yields the correct solution in the central region, and the correct shape in the outer region.

7.3. A Diffusion Test with an Unresolved Boundary Layer

This test problem involves a source-free, two-region sphere ($R = 11$) subjected to an isotropic incident angular flux ($\psi(R, \mu) = 1, \mu < 0$) on the outer boundary. The central region is a thick, pure scatterer (σ_t=σ_s=100), and the outer region is a relatively thin pure absorber (σ_t=2) [7]. The purpose of this test problem is to investigate the influence of the boundary condition on the leading order transport solution in the interior of the diffusive region, given an anisotropic incident angular flux on the purely scattering central region. The problem is solved using a spatial

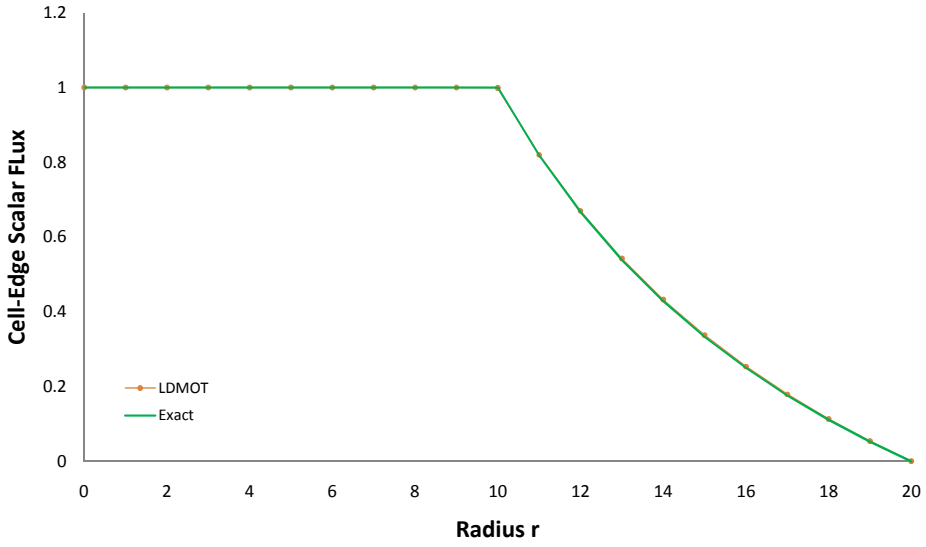

Figure 4. Test Problem 2 Cell-Edge Scalar Flux for the LDMOT Scheme.

Table III. Test Problem 3

Region	Spatial Interval	σ_t	σ_s	q
1	$0 < r < 10$	100	100	0
2	$10 < r < 11$	2	0	0

Table IV. Test Problem 3'

Region	Spatial Interval	σ_t	σ_s	q
1	$0 < r < 10$	100	100	0
2	$10 < r < 11$	4	0	0

mesh with 10 equal-sized cells in each region. Table III contains the problem specification for this test problem.

The flux incident on the sphere is attenuated in the outer absorbing region to create an anisotropic angular flux coming into the central diffusion region (at r=10). This anistropic angular flux has

the following form:

$$\psi(10,\mu) = e^{-\sigma_a(10\mu+\sqrt{11^2-10^2(1-\mu^2)})} \quad \mu < 0\,, \tag{60}$$

where $\sigma_a = 2$ and $\sigma_a = 4$ for Problem 3 and Problem 3', respectively.

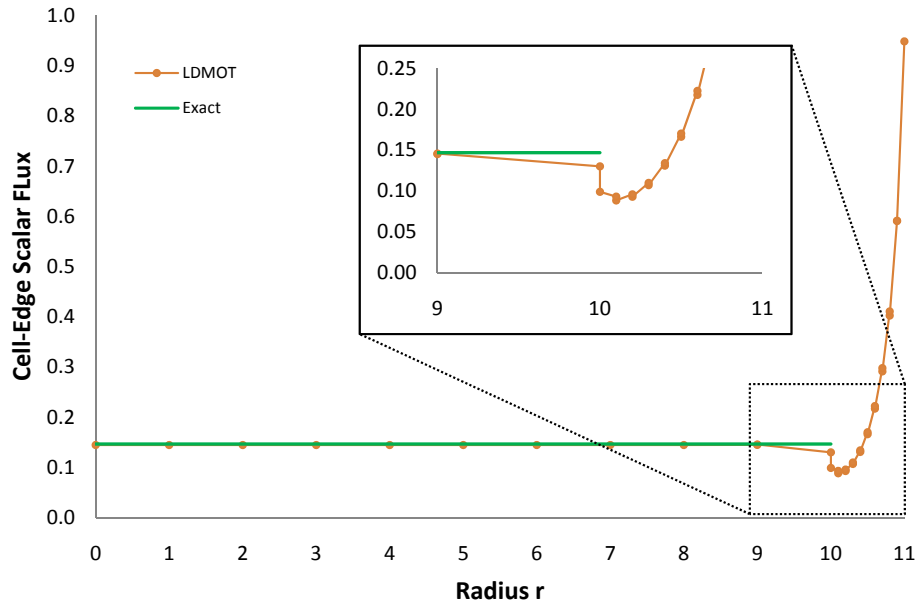

Figure 5. Test Problem 3 Cell-Edge Scalar Flux for the LDMOT Scheme.

The solution in the central domain is constant and is equal to the value of the scalar flux resulting from the asymptotic diffusion boundary condition at r=10 formed by the anisotropic angular flux (Eq. (60)) entering from the pure absorbing subregion.

Figures 5 and 6 contain the results of this test problem. The analytic result for the spatially constant flux in the inner region is 0.14674 found using Eq. (60) for $\sigma_a = 2$. The LDMOT solution is very accurate with a 1.34% relative error.

A second version of this problem (Problem 3'), defined in Table IV, contains a purely absorbing outer region with a larger total cross-section ($\sigma_t = \sigma_a = 4$). In this case the analytic solution of the diffusion problem with the asymptotic boundary condition the inner region has the value of 0.013989 found using Eq. (60) for $\sigma_a = 4$. Figure 6 shows that the relative error in the LDMOT scheme is 1.29%.

7.4. A Set of Tests on the Asymptotic Diffusion Limit

In this test problem, we consider a sequence of homogeneous spheres ($R = 10$) with $\sigma_t = \frac{1}{\varepsilon}$, $\sigma_a = \varepsilon$, and $q = \varepsilon$ [10], with a vacuum outer boundary. The purpose of this problem is to investigate the rate of convergence of the transport solution to the diffusion solution. The numerical solution should approach the leading-order solution predicted by our analysis as ε

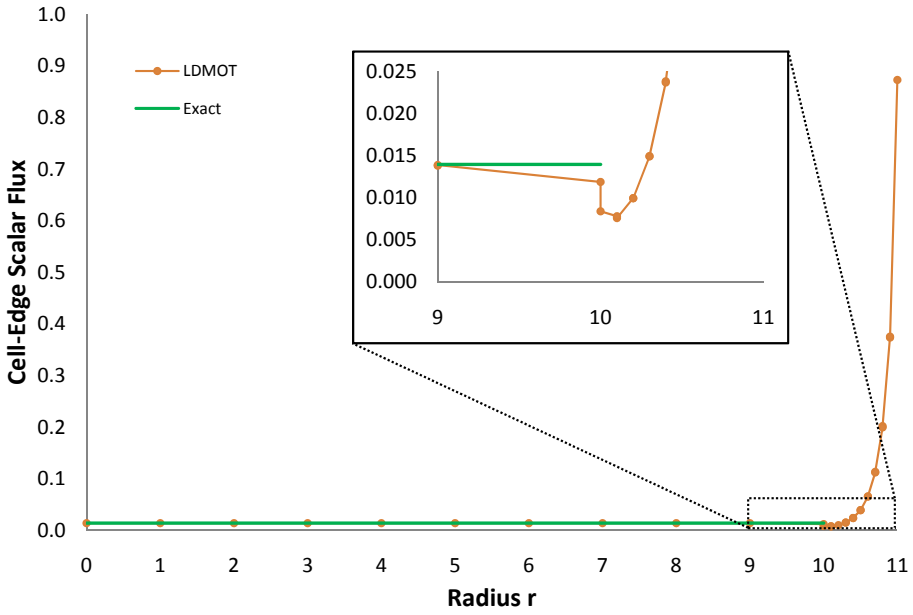

Figure 6. Test Problem 3' Cell-Edge Scalar Flux for the LDMOT Scheme.

approaches zero with an error of $O(\varepsilon)$. We solve each problem with a spatial mesh consisting of 10 uniform cells.

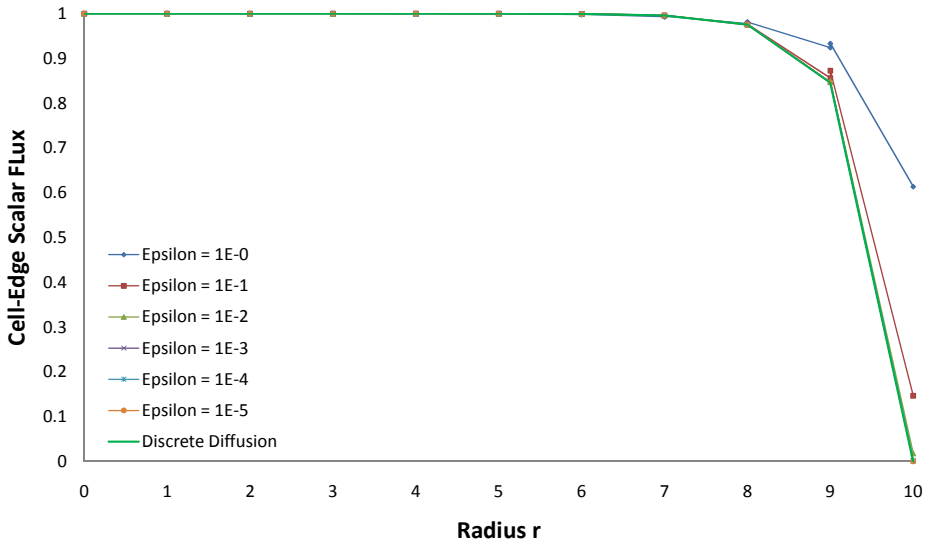

Figure 7. Test Problem 4 Cell-Edge Scalar Flux for the LDMOT.

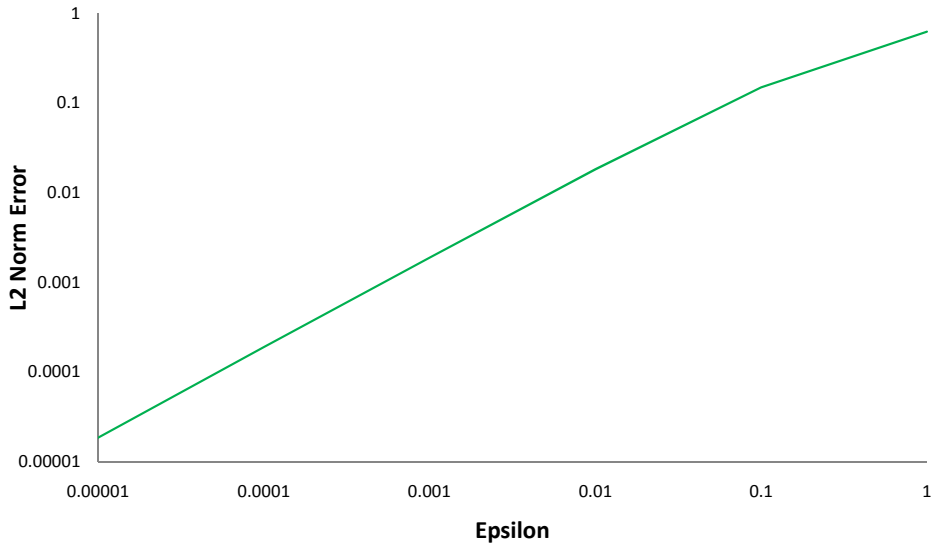

Figure 8. Test Problem 4 L_2 Norm of the Difference Between the LDMOT Transport Solution and the Solution of the Discrete Diffusion Equations.

Table V. Estimated Spectral Radius Comparison

Epsilon	Source Iteration	Diffusion Synthetic Acceleration
$1E-1$	$0.98976067 \pm 5.35E-05$	$0.15078413 \pm 1.02E-01$
$1E-2$	$0.99989655 \pm 5.64E-07$	$0.15964019 \pm 1.05E-01$
$1E-3$	$0.99998564 \pm 1.21E-06$	$0.11300607 \pm 1.19E-01$
$1E-4$	N/A	$0.21546069 \pm 1.32E-01$
$1E-5$	N/A	$0.32981922 \pm 1.59E-01$

Figure 7 shows that the solution from our new linear discontinuous version of the MOT approaches the predicted discrete diffusion solution. As ε approaches zero, the scalar flux solution in the problem interior becomes the infinite medium solution ($\phi = 1$) and the scalar flux on the boundary will be zero. Furthermore Figure 8 shows that the LDMOT transport solution converges to the solution of the discrete diffusion equation at the rate predicted by the analysis ($O(\varepsilon)$).

Table V shows a comparison of the estimated spectral radius for both Source Iteration (SI) and the diffusion synthetic accelerated iterations. As expected, the DSA iterations converge to the same

solutions in many fewer iterations. The DSA makes it possible to run problems with $\epsilon < 1E-3$, where it is prohibitively time consuming to run these problems with just PI (PI $\approx 10^7$ iterations vs. DSA $\approx 10^1$ iterations for $\epsilon = 1E-3$).

7.5. A Test with a Pure Scatterer and Uniform Source

In this test problem, we consider a homogeneous sphere ($R = 10$) of 100 uniform cells radially with $\sigma_t = \sigma_s = q = 1.0$ and a vacuum boundary condition. The purpose of this test problem is to investigate the possibility of a flux dip at the origin of the sphere seen in other discrete-ordinates FEM spherical geometry methods [13]. If the flux dip exists, we would expect that the slope of the flux would changes signs at the origin.

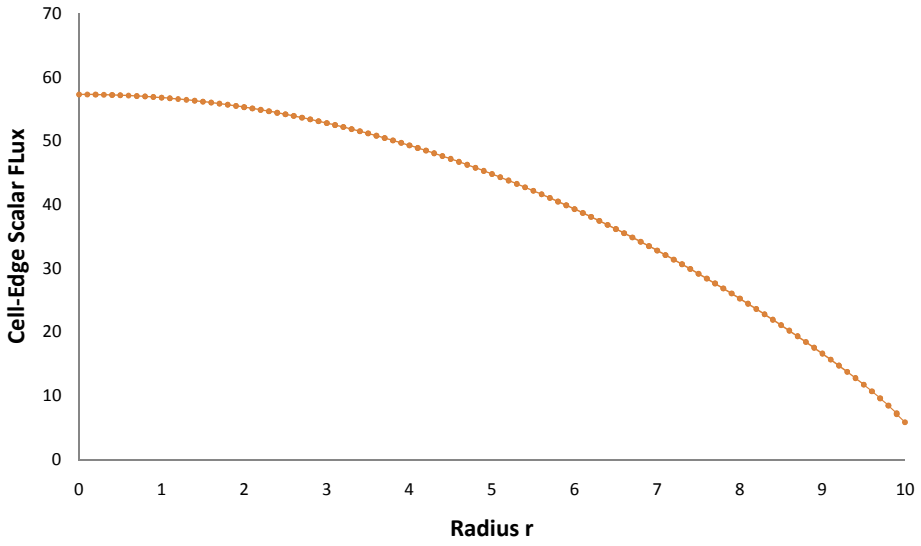

Figure 9. Test Problem 5 Cell-Edge Scalar Flux for the LDMOT.

In this figure, there is no observable flux-dip. Without a proof, however, we consider the existence of a flux dip in the LDMOT an open question.

8. CONCLUSIONS

We have derived, asymptotically analyzed and implemented a new linear discontinuous finite element variant of the spherical geometry method of tubes. The LDMOT transport solution satisfies a reasonable discretization of the diffusion equation with boundary conditions which are accurate approximations of those obtained in the analysis of the analytic spherical geometry transport equation.

The three-point removal term in the discrete diffusion equation satisfied by the LDMOT has the potential to introduce unphysical oscillations in the scalar flux, though we haven't observed this

behavior in the test problems we have included here. This can be alleviated by "lumping" the first moment equation using a procedure developed in the finite element literature. This "lumped" method will have reduced accuracy in optically thin and intermediate regions, but increased robustness in thick diffusive regions.

The transformation of the equation to characteristic form removes two problems with the weighted-diamond approach to the angular discretization: the serial nature of the discretization (angular fluxes must be calculated in a particular order), and the necessity to calculate the solution in the "starting-direction" ($\mu = -1$). It also appears that there is no flux dip at the origin of the sphere for the LDMOT discretization. An analysis of should be performed to further investigate this behavior.

ACKNOWLEDGEMENTS

We thank Dmitriy Anistratov for many helpful discussions in understanding the original work of Nikiforova, Tarasov and Troschiev, This work was supported by a research grant from Lawrence Livermore National Laboratory's' A/X Division.

REFERENCES

[1] T.S. Palmer and M.L. Adams, "Analysis of Spherical Geometry Finite Element Transport Solutions in the Thick Diffusion Limit," *Proc. of the International Topical Meeting of the American Nuclear Society–Advances in Mathematics, Computations, and Reactor Physics*, Pittsburgh, PA, Vol. 5, pp. 21.1 4-1 to 21.1 4-11 (1991).

[2] J. S. Warsa and J. E. Morel, "Solution Algorithms for a P_{N-1} - Equivalent S_N Angular Discretization of the Transport Equation in One-dimensional Spherical Coordinates," *Proc. of the Joint International Topical Meeting on Mathematics and Computations and Supercomputing in Nuclear Applications, M&C + SNA 2007*, Monterey, CA (2007).

[3] A.V. Nikoforova, V.A. Tarasov and V.E. Troshchiev, "Solution of the Kinetic Equations by the Divergent Method of Characteristics," *USSR Comp. Math. and Math. Phys.*, **12**, pp. 251-260 (1972).

[4] M. E. Rising and T.S. Palmer, "An Analysis of the 1-D Spherical Geometry Method of Tubes in the Thick Diffusive Limit," *Trans. Am. Nucl. Soc.*, **98** (2008).

[5] M.E. Rising and T.S. Palmer, "'Moments-Based' Versions of the Spherical Geometry Method of Tubes in Thick, Diffusive Regions," *Nucl. Sci. Eng.*, **160**, pp. 284-301 (2008).

[6] E.W. Larsen, J.E. Morel and W.F. Miller, Jr., "Asymptotic Solutions of Numerical Transport Problems in Optically Thick Diffusive Regimes," *J. Comp. Phys.*, **69**, pp. 283 (1986).

[7] E.W. Larsen and J.E. Morel, "Asymptotic Solutions of Numerical Transport Problems in Optically Thick Diffusive Regimes II," *J. Comp. Phys.*, **83**, pp. 212 (1989). See also "Corrigendum," *J. Comp. Phys.*, **91**, pp. 246 (1990).

[8] S. Chandrasekhar S., *Radiative Transfer*, Dover, New York USA (1960).

[9] M.L. Adams and E.W. Larsen, "Fast Iterative Methods for Discrete-Ordinates Particle Transport Calculations," *Progress in Nuclear Energy*, **40**, pp. 3 (2002).

[10] M.L. Adams, T.A. Wareing,and W.F. Walters, "Characteristic Methods in Thick Diffusive Problems," *Nucl. Sci. Eng.*, **130**, pp. 18 (1998).

[11] W.H. Reed, "The Effectiveness of Acceleration Techniques for Iterative Methods in Transport Theory," *Nucl. Sci. Eng.*, **45**, pp. 245 (1971).

[12] E.W. Larsen, "Unconditionally Stable Diffusion Synthetic Acceleration Methods for the Slab Geometry Discrete-Ordinates Equations. Part I: Theory," *Nucl. Sci. Eng.*, **82**, pp. 47 (1982).

[13] J.E. Morel and G.R. Montry, "Analysis and Elimination of the Discrete-Ordinates Flux Dip," *Trans. Theory and Stat. Phys.*, **13**, pp. 615 (1984).